Heitmann, P., & Uhlig, H. J. (1974) *Acta Biol. Med. Ger. 32*, 565–573.
Heitmann, P., Mollerke, C., & Uhlig, H. J. (1972) *Acta Biol. Med. Ger. 29*, 551–560.
Hsu, C. M., & Cooperman, B. S. (1976) *J. Am. Chem. Soc. 98*, 5657–5663.
Hubner, P. W. A., & Milburn, R. M. (1980) *Inorg. Chem. 19*, 1267–1272.
Janson, C. A., Degani, C., & Boyer, P. D. (1979) *J. Biol. Chem. 254*, 3743–3749.
Jardetzky, O., & Roberts, G. C. K. (1981) *NMR in Molecular Biology*, pp 123–125, Academic Press, New York.
Kirby, A. J., & Varvoglis, A. G. (1967) *J. Am. Chem. Soc. 89*, 415–423.
Knight, W. B., Fitts, S. W., & Dunaway-Mariano, D. (1981) *Biochemistry 20*, 4079–4086.
Knight, W. B., Dunaway-Mariano, D., Ransom, S. C., & Villafranca, J. J. (1984) *J. Biol. Chem. 259*, 2886–2895.
Kostelnik, R. J., & Bothner-By, A. A. (1974) *J. Magn. Reson. 14*, 141–151.
Kunitz, M. (1952) *J. Gen. Physiol. 35*, 423–450.
Kuranova, I. P., Smirnova, E. A., Makhaldiani, V. V., Voronova, A. A., Arutyunyun, E. G., Hohne, W. E., & Hansen, G. (1981) *Dokl. Akad. Nauk SSSR 258*, 1246–1250.
Kuranova, I. P., Terzyan, S. S., Voronova, A. A., Smirnova, E. A., Vainstein, B. K., Hohne, W., & Hansen, G. (1983) *Bioorg. Khim. 9*, 1611–1619.
Moe, O. A., & Butler, L. G. (1972) *J. Biol. Chem. 247*, 7308–7314.
Palmer, A. R., Bailey, D. B., Benske, W. D., Cardin, A. D., Yang, P. P., & Ellis, P. D. (1980) *Biochemistry 19*, 5063–5070.
Rapoport, T. A., Hohne, W. E., Heitmann, P., & Rapoport, S. (1973) *Eur. J. Biochem. 33*, 341–347.
Reed, G. H., & Bock, J. L. (1979) *Biochem. Biophys. Res. Commun. 86*, 460–463.
Ridlington, J. W., & Butler, L. G. (1972) *J. Biol. Chem. 247*, 7303–7307.
Springs, B., Welsh, K. M., & Cooperman, B. S. (1981) *Biochemistry 20*, 6384–6391.
Welsh, K. M., Armitage, I. M., & Cooperman, B. S. (1983a) *Biochemistry 22*, 1046–1054.
Welsh, K. M., Jacobyansky, A., Springs, B., & Cooperman, B. S. (1983b) *Biochemistry 22*, 2243–2248.

X-ray Analysis of the Kinetics of *Escherichia coli* Lipid and Membrane Structural Transitions†

Jean Luc Ranck,* Lucienne Letellier, Emanuel Shechter, Brigitte Krop, Pierre Pernot, and Annette Tardieu

ABSTRACT: Synchrotron radiation was used to follow the time course of the transitions, induced by temperature jump, in *Escherichia coli* membranes and their lipid extracts isolated from a fatty acid auxotroph grown with different fatty acids. We measured the relaxation times associated with the phase transitions as well as with the conformational transition of the hydrocarbon chains and observed different behavior as a function of chemical composition. Relaxation times of about 1–2 s were found at a hexagonal to lamellar phase transition and within a lamellar phase whose parameters display important variations with temperature when the conformational transition takes place. On the other hand, no delay was observed for a phase transition where large lipid or water diffusion was not needed. We have shown that phase transitions and conformational transitions are, to a large extent, uncoupled and that the relaxation times corresponding to the latter transition could be related to the size of the ordered domains. In all cases, the order to disorder conformational transition is more rapid than the disorder to order transition. Finally, the relaxation times of the disorder to order transition observed with the membranes and with their lipid extracts were found to be strongly correlated, indicating that the proteins do not play a role in this transition.

Lipid–water systems are known to exhibit a remarkable polymorphism as a function of temperature and water content (Luzzati & Tardieu, 1974). In addition, the hydrocarbon chains of the lipids undergo reversible, temperature-dependent transitions between disordered (type α) and partially ordered (type β, β') conformations (Tardieu et al., 1973; Ranck, 1983). Such systems have been extensively studied by using a variety of physical techniques (X-ray diffraction, calorimetry, spectroscopy, etc.) and a number of phases, and a variety of hydrocarbon chain conformations are now fairly well characterized [for recent reviews, see Zannoni et al. (1983), Kimmich et al. (1983), Hemminga (1983), and Ranck (1983)].

In the past, we have used high-angle X-ray diffraction to investigate the behavior as a function of temperature of various cytoplasmic membranes and lipid extracts isolated from an *Escherichia coli* unsaturated fatty acid auxotroph. This enabled us to establish correlations between structural, morphological, and physiological properties of these systems (Shechter et al., 1974; Letellier et al., 1977). In the present study, the earlier work is extended to an analysis of the time course of the transition phenomena induced by temperature jumps.

First, we recorded both high- and low-angle diffraction patterns for the lipid extracts in the presence of water. The structure of the phases observed as a function of temperature

† From the Centre de Génétique Moléculaire, C.N.R.S., 91190 Gif-sur Yvette, France (J.L.R., B.K., and A.T.), and the Laboratoire des Biomembranes, Bat. 433 (L.L. and E.S.), and L.U.R.E., Bat. 209c (P.P.), Université Paris-Sud, 91405 Orsay, France. *Received January 9, 1984.*

0006-2960/84/0423-4955$01.50/0

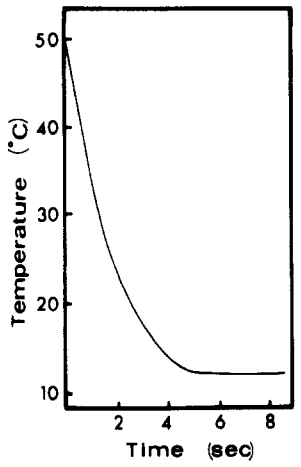

FIGURE 1: Typical temperature jump.

(long-range order) can thus be determined in addition to the conformation of the hydrocarbon chains (short-range order) previously analyzed. Second, and more importantly, dynamic, as well as static, studies were performed. The high X-ray fluxes from a Synchrotron radiation source and a specially designed temperature-jump apparatus (T-jump apparatus) allowed us to determine the time required for the various transitions to take place, within both the cytoplasmic membranes and the isolated lipid extracts.

Materials and Methods

Apparatus. (*A*) *X-ray Experiments.* X-ray diffraction studies were performed with the small-angle camera, described in detail elsewhere (Koch et al., 1982), at the Synchrotron Radiation Laboratory, L.U.R.E., Orsay, France.

Low-angle diffraction data were obtained with a linear position sensitive detector (PSD) with delay line position encoding (Gabriel, 1977). High-angle diffraction data were recorded with a multiwire detector (Pernot et al., 1983). In both cases, the same data acquisition system, specifically designed by one of us (P.P.) for kinetic experiments, was used. Up to 35 spectra of 512 channels could be sequentially recorded according to a preprogrammed time sequence. Once the acquisition was completed, the data were stored on a PDP disk.

(*B*) *T-Jump Apparatus.* An X-ray-transparent sample cell (area, 4 mm × 2 mm; thickness, 0.5 mm) has built-in Peltier elements whose rapid current inversion allows T jumps of several tens degrees centigrade to be achieved. The cooling rate varies from 10 to 20 °C/s, while the heating rate can be as high as 30 °C/s. The speed may vary slightly as a function of the temperature range of the jump, yet a given T jump may be repeated with perfect reproducibility. A typical T jump is shown in Figure 1. During an actual X-ray experiment, the temperature can only be measured outside the sample. Control experiments have shown that the times required to reach a given temperature during a T jump, measured inside and outside the sample cell, differ at most by about 300 ms. This sets the lower limit of the calculated delays (see below).

Experimental Procedures. High- or low-angle X-ray spectra were first recorded in a static way as a function of the temperature. The recording time at each temperature was varied between 1 s and 1 min depending upon the diffracted intensity. From these spectra, the domain of existence of the various phases and the transition temperatures were determined, and the extreme temperatures of the T jumps were chosen so as to cover the transition of interest. Kinetic experiments were then performed on the same sample by starting simultaneously the T jump and the data acquisition. We used the following recording time sequence: 10 spectra of 100 ms, 20 spectra of 200 ms, and 5 spectra of 600 ms for each T jump. To improve the counting statistics, 5–20 T-jump cycles were performed on each sample. It is worth mentioning that lipid and membrane transitions are reversible phenomena and that the systems are able to withstand repeated cycles. Static spectra taken, at the same temperature, before and after a series of T-jump cycles were perfectly superposable.

The data presented here are raw data. They are unsmoothed and uncorrected for background scattering, collimation distortions, or detector response.

Samples. Cytoplasmic membranes and the lipid extracts were prepared as previously described (Shechter et al., 1974).

The samples used were pellets of the cytoplasmic membranes isolated from an *E. coli* unsaturated fatty acid auxotroph grown on two different unsaturated fatty acids, elaidic acid ($\Delta^{9,trans}$ C18:1) and oleic acid ($\Delta^{9,cis}$ C18:1). The membranes are specifically enriched in these unsaturated fatty acids (Shechter et al., 1974) and referred to in the following as elaidate membranes and oleate membranes, respectively.

The lipids were extracted from the isolated membranes and mixed with water in about a 1:1 (w/w) ratio approximating the water content of the membrane pellets. We refer to them as elaidate lipids and oleate lipids, respectively.

The fatty acid composition of elaidate lipids and membranes was 2% C12:0, 16% C14:0, 10% C16:0, and 72% trans C18:1. The fatty acid composition of oleate lipids and membranes was 1% C12:0, 16% C14:0, 36% C16:0, 40% cis C18:1, 5% cis C18:2, and 2% unknown (Shechter et al., 1974).

Lipids were also extracted from membranes isolated from *Bacillus subtilis.* They contain about 60% branched fatty acids and 40% saturated ones (Legendre et al., 1980).

Results

Static Analysis. The first step of the data analysis was to determine the structural characteristics of each sample as a function of temperature.

The high-angle part of the X-ray diffaction pattern gives information on the organization of the hydrocarbon chains. In all systems, at sufficiently high temperature, a broad band was observed around 1/4.5 $Å^{-1}$, characteristic of a disordered conformation of the hydrocarbon chains (α conformation) (Luzzati & Tardieu, 1974). Whith decreasing temperature, for *E. coli* lipids and membranes there appeared, superimposed on this broad band, a sharp reflection centered at 1/4.2 $Å^{-1}$, indicating the presence of stiff and parallel hydrocarbon chains, oriented at right angles to the plane of the lamellae and organized with rotational disorder on a two-dimensional hexagonal lattice (β conformation) (Luzzati & Tardieu, 1974). This situation is common in lipids with heterogeneous fatty acid composition and corresponds to the temperature-induced segregation, within the lamellae, of domains with hydrocarbon chains in either α or β conformations (Ranck, 1983). This mixed organization of the hydrocarbon chains is usually referred to as $\alpha\beta$ (Figure 2). The integrated intensity of the 1/4.2-$Å^{-1}$ reflection is proportional to the amount of ordered hydrocarbon chains within the lamellae (Shechter et al., 1974).

The high-angle data reported here confirm the results previously described (Shechter et al., 1974; Legendre et al., 1980). Thus, (i) the order–disorder transition is qualitatively similar for a given membrane and for the corresponding total lipid extract, the temperature range of the transition being similar (although not identical) for a given membrane and for the corresponding lipid extract (Figure 2), (ii) only a fraction of the lipid chains becomes ordered at the low-temperature

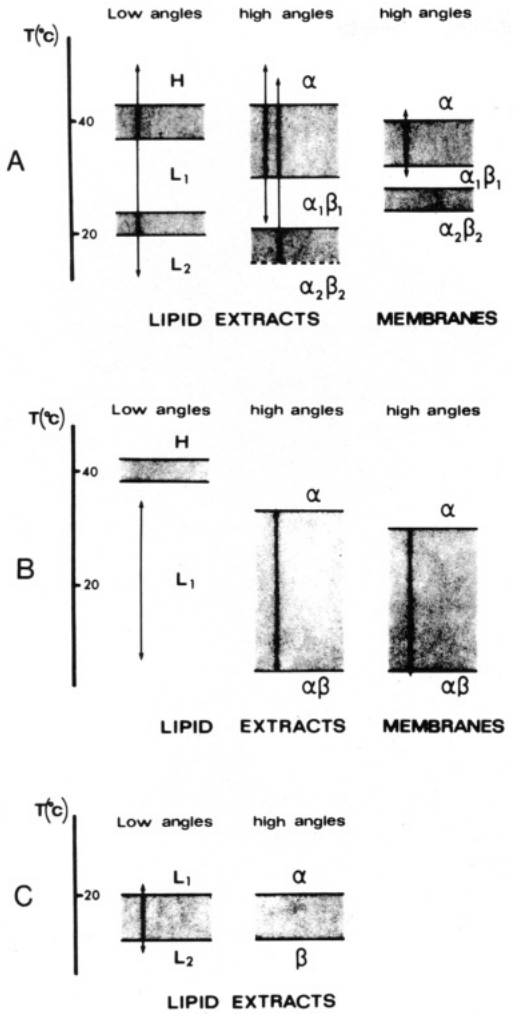

FIGURE 2: "Phase diagrams" of the various systems studied. The amount of water was on the order of 60% (not accurately determined). At low angles, the regions indicated in grey correspond to temperature domains where mixtures of phases were observed. At high angles, the grey regions correspond to temperature domains where the amount of ordered chains varied. The arrows indicate the extreme temperatures of the T jumps that have been performed. (A) Elaidate lipids and membranes. Note that the main α to β transition occurs at the H–L1 transition. $\alpha_1\beta_1$ and $\alpha_2\beta_2$ correspond to different ratios of ordered (β) and disordered (α) chains. (B) Oleate lipids and membranes. (C) *Bacillus subtilis* lipids.

end of the transition, (iii) the amount of ordered lipids is larger for a given lipid extract than for the corresponding membrane, and (iv) the temperature range of the transition is dependent upon the fatty acid composition and is thus different for different membranes (or different lipid extracts).

The actual range of the transitions from the disordered conformation (α) to the partially ordered conformation ($\alpha\beta$) is displayed in Figure 2. It includes between 25 and 45 °C for elaidate membranes and lipids and between 10 and 30 °C for oleate membranes and lipids. These results clearly indicate that while proteins present in the membrane affect the amount of lipids involved in the order–disorder conformational transition, they do not greatly disturb the temperature range of that transition.

In the case of *Bacillus subtilis* lipids and membranes, as a consequence of the presence of branched fatty acids, a broad reflection at $1/4.3$ Å^{-1} is observed at low temperature instead of the sharp $1/4.2$-Å^{-1} reflection observed with *E. coli* lipids and membranes (Legendre et al., 1980). The order to disorder transition was found to occur between 5 and 20 °C for the lipid extracts. Although it occurs in the same temperature range, the transition within the membranes could not be accurately analyzed because of the low intensity of the $1/4.3$-Å^{-1} reflection.

Low-angle X-ray diffraction patterns recorded as a function of temperature on the lipid extracts display sharp reflections whose relative spacings allowed us to determine the type of the phases involved. From these spacings and their evolution as a function of temperature, all the phases described below behave as pure phases with no water in excess. The results are displayed in Figure 2.

Elaidate lipids display, as a function of decreasing temperature, a hexagonal phase, then a first lamellar phase (L1), and then a second lamellar phase (L2) having a different repeat distance. The main order–disorder transition of the hydrocarbon chains takes place at the H–L1 transition. Within L1, and as a function of decreasing temperature, the amount of ordered chains is first seen to vary slightly and then remains constant. An additional fraction (5–10%) of the lipids becomes ordered at the L1–L2 transition. At the low end of this transition, about 95% of the hydrocarbon chains are ordered (Shechter et al., 1974).

Oleate lipids display, as a function of decreasing temperature, a hexagonal and a lamellar phase (L1). The order to disorder transition of the hydrocarbon chains takes place within L1. The repeat distance of L1 is seen to evolve continuously during this transition. At the lower end of the transition, about 50% of the hydrocarbon chains are ordered (Shechter et al., 1974).

Lipids isolated from *Bacillus subtilis* membranes display, as a function of decreasing temperature, two lamellar phases (L1 and L2) having different, although close, repeat distances. The order to disorder transition of the hydrocarbon chains takes place during the phase transition.

The relationships between long-range and short-range order are therefore different in the three systems presented above: the main disorder to order conformational transition occurs at a hexagonal to lamellar phase transition for elaidate lipids, within a lamellar phase for oleate lipids, and at a lamellar–lamellar phase transition for *B. subtilis* lipids.

Kinetic Analysis. The T jumps that were studied are displayed schematically in Figure 2.

We first verified that the initial and final spectra were identical with the corresponding ones taken statically. Then, the sequence of events observed as a function of time after initiation of the temperature jump was compared to that observed in the static experiments as a function of temperature. We observed that, for both low and high angles, each dynamic spectrum could be correlated with a static one having essentially similar peak positions, widths, and intensities (minor differences could have escaped us as the counting statistic is limited in dynamic experiments). The evolution of some X-ray spectra as a function of time is shown in Figure 3.

However, we observed that the spectra recorded at a given sample temperature during the temperature jump may differ from the spectra recorded at the same temperature in static experiments. This indicates that the transitions are not instantaneous. The comparison of static and dynamic data may thus lead to the determination of the time required for the various transitions to take place. Operationally, we expressed this time in terms of a delay which was quantified in the following way. For each sample, we searched for the parameter that was varying most as a function of temperature, the peak position or the peak integrated intensity for instance, and plotted for the kinetic data the evolution of this parameter vs. *time*. From the static experiments, we can plot the evolution

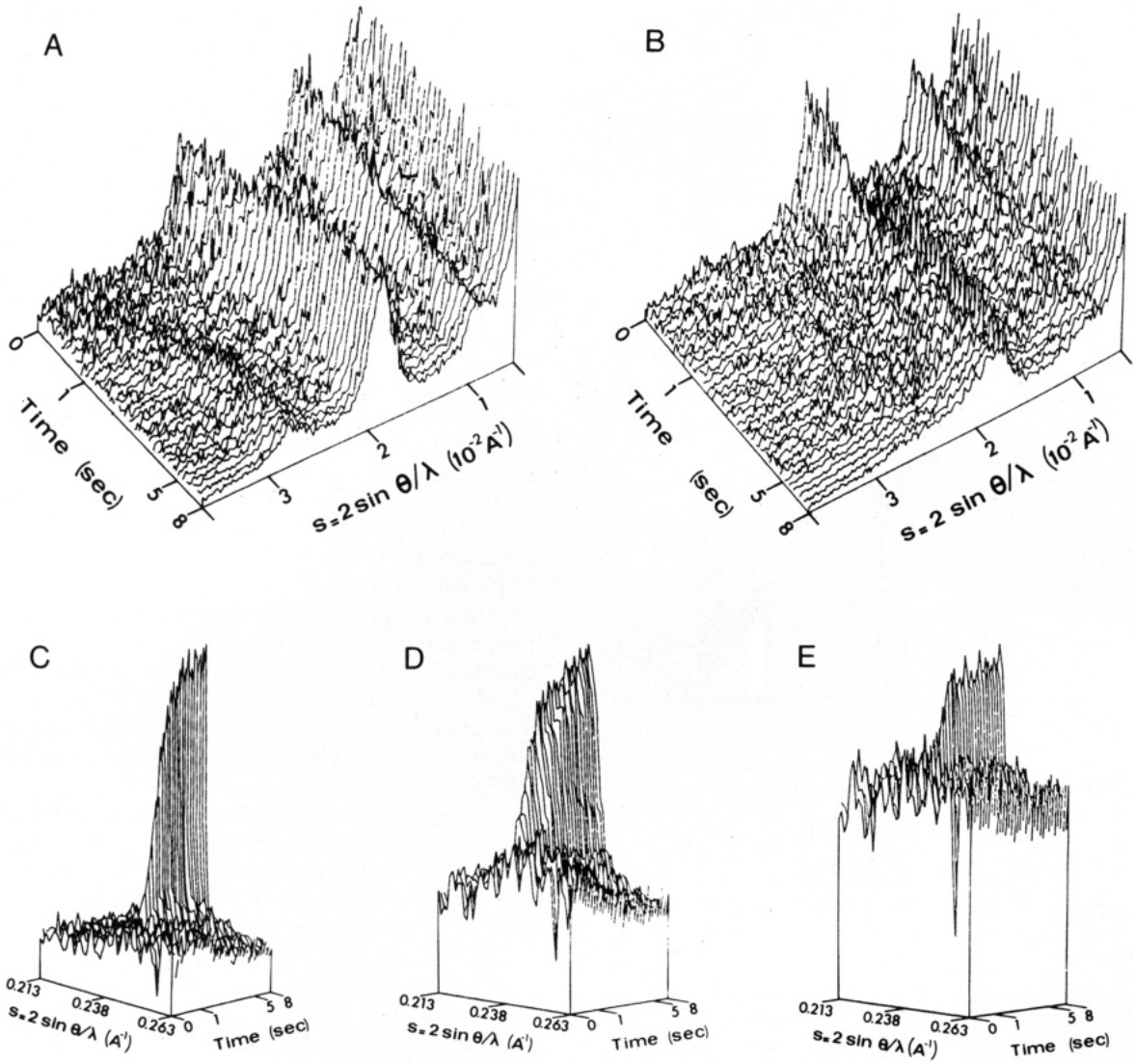

FIGURE 3: Examples of raw X-ray data recorded as a function of time. The 35 spectra were normalized to equal recording time. (A) Low-angle data recorded with oleate lipids. The two main peaks are the second and third order of a lamellar repeat. The repeat distance varies from 96 Å at high temperature up to 107 Å at low temperature. The T jump was from 35 to 7 °C. (B) Low-angle data recorded with *B. subtilis* lipids. The main peak is the second order of a lamellar repeat of 105 Å. The repeat distance is about the same at low temperature. Note, however, the broadening of the reflections at low temperature (that hinders precise determination of the repeat distance). The T jump was from 22 to 10 °C. (C) High-angle data recorded with elaidate lipids. The T jump was from 47 to 15 °C. (D) High-angle data recorded with oleate lipids. The T jump was from 33 to 5 °C. (E) High-angle data recorded with elaidate membranes. The T jump was from 42 to 30 °C. Note that in panels C–E the relative intensity of the 1/4.2-Å^{-1} reflection vs. background provides an estimate of the amount of ordered chains present in the X-ray beam during each experiment.

of this desired parameter vs. *temperature*. Since during kinetic experiments we also recorded the evolution of *temperature* vs. *time* during the T jump (Figure 1), it is therefore possible to translate the evolution of the desired parameter recorded as a function of temperature during the static experiments into a pseudo evolution as a function of time. We thus obtained two curves of intensity vs. time, one equivalent to the variation of the signal that would be obtained during the temperature jump if the sample structure was at all times that corresponding to the sample temperature ("static" curve) and the other being the experimental curve ("dynamic" curve). The curves, normalized, were plotted on the same figure (see Figures 4–6). We define the delay as the time difference between both curves at midtransition. The data are summarized in Table I. Dynamic data can also be plotted as a function of the time difference between the static and dynamic values. Examples of such representations are given in Figure 7.

Elaidate. At low angles, we followed the integrated intensities of different parts of the X-ray spectra that contain characteristic features of the various phases. These regions are indicated in Figure 4A; the evolution of region I displayed in Figure 4B,C shows the disappearance of the hexagonal phase during an H to L2 jump and its appearance during the reverse jump; the evolution of region IV displayed in Figure 4D shows the appearance and disappearance of the L1 phase during the H to L2 jump.

Table I: Midtransition Delays (in Seconds) Calculated from the Data of Figures 4–6[a]

	elaidate			oleate			*B. subtilis*
	lipids		membranes,	lipids		membranes,	lipids,
	la	ha	ha	la	ha	ha	la
down	0.9 (H to L1)	1.8	0.9	1.0	0	0	0
up	0.6	0.6	0	0.4	0	0	0

[a] Down and up correspond to temperature jumps starting respectively from high and low temperatures (see Figure 2 for the T jumps performed). Abbreviations: la, low angles; ha, high angles.

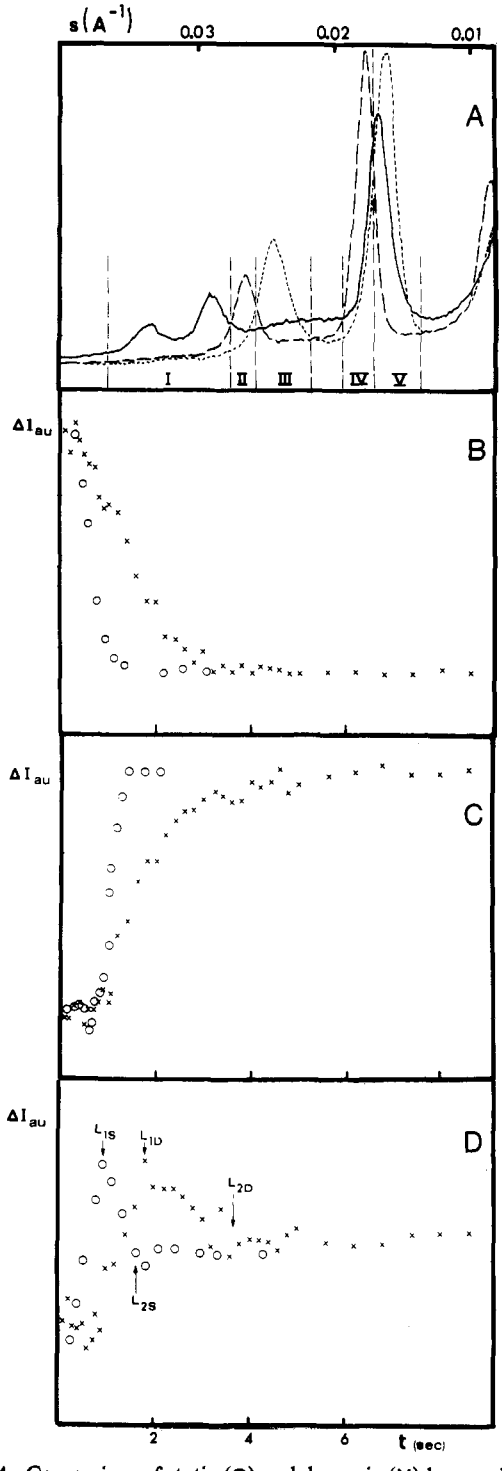

FIGURE 4: Comparison of static (O) and dynamic (×) low-angle data for elaidate lipids. See the text for the definition of static and dynamic data. (A) Low-angle X-ray spectra (static) at various temperatures as a function of s ($s = 2 \sin \theta/\lambda$): (—) hexagonal phase; (- - -) L1 phase; (···) L2 phase. The spectrum has been divided into five regions (I–V). Region I is sensitive to the H to L1 transitions and has been used to determine the delays involved during these transitions. Region IV is sensitive to the appearance and disappearance of the L1 phase and has been used to determine the delay involved in the L1 to L2 phase transition. Time dependence of the integrated intensity (in arbitrary units) for region I (H to L1 phase transition) (B), region I (L1 to H phase transition) (C), and region IV (L1 to L2 phase transition) (D). The arrows indicate when pure L1 and L2 phases are observed, either in static (s) or in dynamic (d) experiments. The temperature jump was from 50 to 12 °C (B and D) or from 12 to 50 °C (C).

From these data, the H to L1 phase transition displays a midtransition delay of 0.9 s. The maximum intensity of the

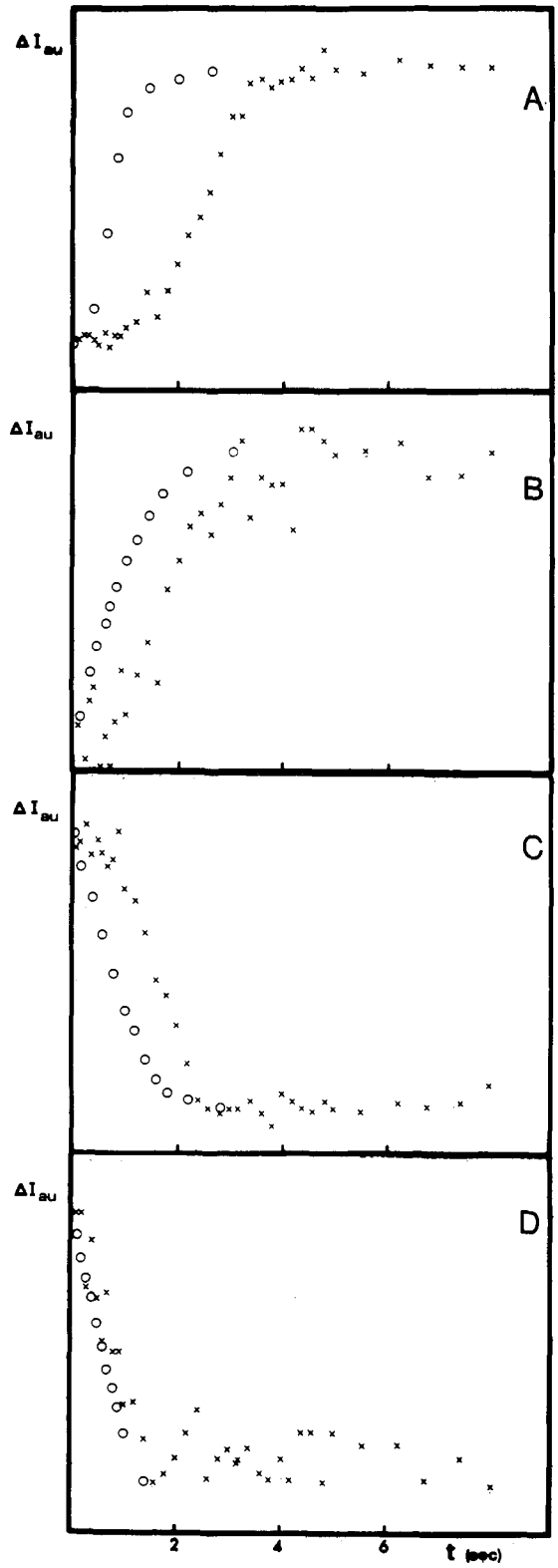

FIGURE 5: Comparison of static (O) and dynamic (×) high-angle data for elaidate lipids and membranes. The parameter followed in all cases was the integrated intensity (in arbitrary units) of the 1/4.2-Å^{-1} reflection. (A) Elaidate lipids; T jump from 47 to 15 °C. (B) Elaidate membranes; T jump from 42 to 30 °C. (C) Elaidate lipids; T jump from 15 to 47 °C. (D) Elaidate membranes; T jump from 30 to 42 °C.

L1 reflections is observed after some 2 s, and the additional time required to achieve the L1 to L2 transition is about 1.6 s. The L1 to H phase transition displays a midtransition delay of 0.6 s. Note that the process seems to slow down as a function of time and to involve at least two relaxation times (better seen in Figure 7). The transition is complete after

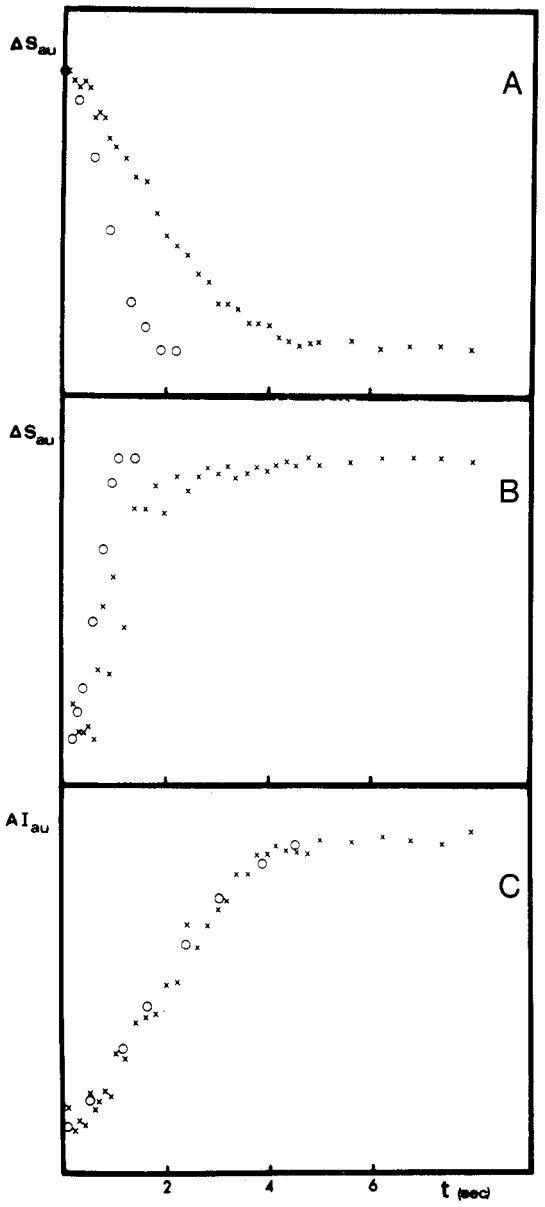

FIGURE 6: Comparison of static (O) and dynamic (×) low- and high-angle data for oleate lipids. At low angles, the parameter followed was the position of a given lamellar reflection; at high angles, the parameter followed was the integrated intensity of the 1/4.2-Å^{-1} reflection. (A) Low-angle data; T jump from 35 to 7 °C. (B) Low-angle data; T jump from 7 to 35 °C. (C) High-angle data; T jump from 35 to 5 °C.

about 5 s. The L2 to L1 phase transition was not followed. Similar results were obtained from the analysis of regions II, III, and V (data not shown).

From high-angle data, the disorder to order conformational transition of the hydrocarbon chains that accompanies the H to L1 phase transition displays a midtransition delay of 1.8 s (Figures 5A and 7), which is larger than the H to L1 delay observed with the low angles. The transition is observed after a lag time. This may be explained in terms of two successive events taking place. Indeed, a hexagonal phase cannot accommodate ordered hydrocarbon chains; thus, the phase transition from H to L1 has to be completed before the ordering of the chains may take place. We conclude, therefore, that the delays corresponding to these two kinds of events are additive and that the ordering, per se, of the hydrocarbon chains in the lamellar phase displays a midtransition delay of about 1 s. The small additional ordering of the hydrocarbon chains which accompanies the L1 to L2 phase transition could

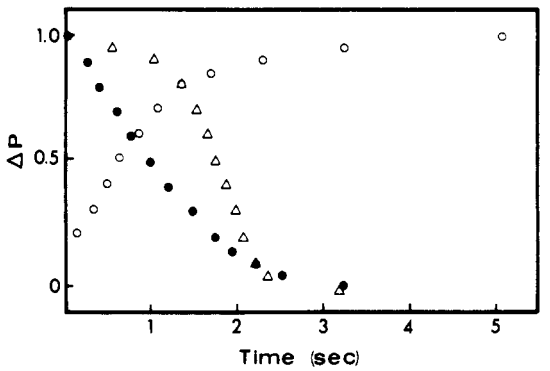

FIGURE 7: To "eliminate" the time required to achieve the temperature jumps, the dynamic data (ΔP stands for the normalized variation of the parameter that was followed during the experiment) can also be plotted as a function of the time difference between static and dynamic data. Examples of such representations, where the experimental data have been smoothed, are given here. The midtransition delay thus corresponds to the time required by ΔP to reach 50%. (O) Corresponds to the data of Figure 4C; (△) data of Figure 5A; (●) data of Figure 6A.

not be detected kinetically. Finally, the order to disorder transition appears to be faster; yet a small delay of about 0.6 s is observed (Figure 5C).

The disorder to order delay observed for elaidate membranes (under conditions where no hexagonal to lamellar phase transition occurs, of course) is 0.9 s (Figure 5B), identical with the one observed with the lipid extracts. No delay was detected for the order to disorder transition (Figure 5D).

Oleate. Oleate lipids do not diplay a phase transition in the temperature range where the disorder to order transition takes place. However, the repeat distance of the lamellar phase is continuously and significantly evolving in this temperature range. The evolution of the peak positions displays a midtransition delay of 1.0 and 0.4 s as a function of decreasing and increasing temperature, respectively (Figure 6A,B). In both cases, the process seems to slow down as a function of time. The transitions are complete after about 4.5 s (Figure 7).

No delay was observed for the disorder to order transition, neither for the lipids (Figure 6C) nor for the membranes (not shown). Thus, the disorder to order transition and the evolution of the lamellar phase appear uncoupled.

Bacillus subtilis. No delay was observed during the temperature jump following the L1 to L2 phase transition or vice versa (not shown). The disorder to order transition could not be followed kinetically as the signal was too small.

Discussion

The use of synchrotron high-X-ray fluxes combined with a temperature-jump apparatus has made it possible, for the first time, to determine some of the relaxation times associated with phase transitions or conformational transitions of membrane lipids and to demonstrate rather different behavior as a function of hydrocarbon chain composition.

Our present analysis is rather coarse and limited to that of the changes of a few parameters: peak positions or integrated intensities. The counting statistics forbid a finer analysis that could be obtained by, for example, analysis of the change in width of the reflections or in the relative intensities of the low-angles peaks. Also, some transitions were too fast to be followed with our present equipment. In turn, such a coarse analysis does not require the consideration of effects like possible temperature heterogeneity due to sample size, thermal conductivity, or specific heat of the sample, which could play a role at a finer analysis level.

The relaxation times associated with the long-range organization of the lipids seem to be well correlated, as expected, with the extent of underlying structural changes. The H to L1 transition of elaidate lipids or the large evolution of the L1 phase of oleate lipids (10% change in the repeat distance), that involve large lipid and water rearrangements, has a relaxation time on the order of 1.0 s, and we have seen that some seconds are needed for the transition to be achieved. The L1 to L2 phase transition of *B. subtilis* lipids, where similar repeat distances are observed, takes place without measurable delay. The results obtained with elaidate and oleate lipids seem to indicate that several mechanisms are responsible for the observed time course of the transitions. Comparison with the results obtained with *Bacillus subtilis* lipids suggests that lipid and/or water diffusion over large distances is a limiting factor in the rate of the transition. Kinetic experiments as a function of water content would probably help in the analysis of such phenomena.

The relaxation times associated with the short-range order of the hydrocarbon chains were shown to be relatively independent of the relaxation times associated with long-range order. Thus, no delay was observed for the disorder to order transition of oleate lipids while the establishment of long-range order requires a delay. On the other hand, besides the delay needed for the H to L1 phase transition, an additional delay is required for the disorder to order transition of elaidate lipids to take place.

In the membranes, the presence of proteins does not introduce any significant additional delay in the conformational transition of the lipids. A similar delay is observed for the disorder to order transition of both elaidate membranes and elaidate lipids as well as for both oleate membranes and oleate lipids. This result indicates that although the proteins affect the amount of lipids taking part in the disorder to order transition, they do not significantly modify the time course of the disorder to order conformational transition of the lipids, which suggests that the proteins do not interact with the lipids that undergo the conformational transition.

The delay for the disorder to order transition has been shown to be rather different for elaidate lipids (or membranes) and oleate lipids (or membranes), 1.0 s and no delay, respectively. That difference might be the consequence of the different sizes of the ordered domains in both cases. Large ordered domains have been demonstrated by freeze–fracture electron microscopy for elaidate membranes and much smaller domains for oleate membranes (Shechter et al., 1974). The limiting step for the disorder to order transition could thus be related to domain growth and/or nucleation. The existence of large domain size could also explain why the order to disorder transition of elaidate lipids is not instantaneous, albeit faster than the disorder to order one. Finally, it should be stressed that the existence of a delay is not related to the absolute amount of lipids taking part in the transition: the amount of ordered lipids is about the same in elaidate membranes that display a delay (55%) and in oleate lipids that do not (50%).

Finer analysis would require higher X-ray intensities and faster temperature-jump equipment in order to improve the counting statistics and to detect faster transitions. The data presented here demonstrate the potential of such studies.

Acknowledgments

We thank J. C. Dedieu for expert drawing of the figures.

Registry No. Elaidic acid, 112-79-8; oleic acid, 112-80-1.

References

Gabriel, A. (1977) *Rev. Sci. Instrum. 48*, 1303–1305.

Hemminga, M. A. (1983) *Chem. Phys. Lipids 32*, 323–383.

Kimmich, R., Schnur, G., & Schevermann, A. (1983) *Chem. Phys. Lipids 32*, 271–322.

Koch, M. H. J., Stuhrmann, H. B., Vachette, P., & Tardieu, A. (1982) in *Uses of Synchrotron Radiation in Biology* (Stuhrman, H. B., Ed.) pp 223–253, Academic Press, New York.

Legendre, S., Letellier, L., & Shechter, E. (1980) *Biochim. Biophys. Acta 602*, 491–505.

Letellier, L., Moudden, H., & Shechter, E. (1977) *Proc. Natl. Acad. Sci. U.S.A. 74*, 452–456.

Luzzati V., & Tardieu, A. (1974) *Annu. Rev. Phys. Chem. 25*, 79–94.

Pernot, P., Kahn, R., Fourme, R., Leboucher, P., Million, G., Santiard, J. C., & Charpak, G. (1982) *Nucl. Instrum. Methods 201*, 145–151.

Ranck, J. L. (1983) *Chem. Phys. Lipids 32*, 251–270.

Shechter, E., Letellier, L., & Gulik-Krzywicki, T. (1974) *Eur. J. Biochem. 49*, 61–76.

Tardieu, A., Luzzati, V., & Reman, F. C. (1973) *J. Mol. Biol. 75*, 711–733.

Zannoni, C., Arcioni, A., & Cavatorta, P. (1983) *Chem. Phys. Lipids 32*, 179–250.